This article has been accepted for publication in a future issue of this journal, but has not been fully edited. Content may change prior to final publication. Citation information: DOI 10.1109/TSTE.2019.2935156, IEEE Transactions on Sustainable Energy

Torque Oscillations Cancellation Targets of a Doubly Fed Induction Machine Operating with Unbalanced and Distorted Grid

Grzegorz Iwanski, *Senior Member, IEEE*, Tomasz Luszczyk, Mateusz Piwek

***Abstract* — The paper focuses on the method of vector control of a doubly fed induction machine connected to the unbalanced power network with simultaneous grid voltage harmonics distortions. As the instantaneous values of torque and the q_s component of power are independent, torque oscillations during grid voltage harmonics can be achieved for different waveforms of q_s power, so a different shape of stator current can be reached at this state. Thus, alternative control targets giving non-oscillatory electromagnetic torque are analyzed and realized in the control. The commanded variables are electromagnetic torque T_{em} and alternatively, the q_s component of stator instantaneous power or a new variable z_s calculated in the same way as the q_s component of power but the amplitudes of each voltage harmonics are reduced *k*-times, where *k* is the harmonic order. The paper discusses how reference stator current vector components can be calculated for each type of torque oscillations cancellation target. The analysis is complemented with a simulation of a 2MW model and laboratory tests of a small power machine.**

***Index Terms* — AC generators, power generation control, induction generator.**

I. Introduction

THE main problem of the grid connected doubly fed induction generator DFIG are symmetrical or asymmetrical voltage sags. Fast change of the stator (grid) voltage and a large amount of negative sequence induce high voltage on the rotor side and make it necessary to enable rotor circuit protections (crowbars) to damp the machine flux and to protect the rotor power converter against too high induced voltage [1]-[3]. During grid voltage asymmetry several targets are possible such as constant *pq* components of stator power, torque oscillations cancellation, symmetrical stator current, sinusoidal rotor current, and constant p_s component of stator power at sinusoidal stator current. Both constant p_s power targets provide enormously high torque oscillations, so these targets are inadequate for most electromechanical systems, especially for wind turbines with gearboxes. Additionally, a constant *pq* components target causes an unacceptable level of stator current harmonics.

The methods aimed at different control targets during grid voltage imbalance are widely discussed in the literature [4]-[6], whereas only a few publications [7]-[8] pay special attention to grid voltage harmonics and compensation of torque oscillations caused by grid voltage harmonics. The influence of harmonics on torque oscillations production has been thoroughly analyzed in [9]. Four main targets have been proposed, i.e, sinusoidal rotor current (*Target I*), symmetrical sinusoidal stator current (*Target II*), constant *pq* components of stator instantaneous power (*Target III*), and torque oscillations cancellation with simultaneous constant q_s component of instantaneous stator power (*Target IV*).

Although symmetrical, sinusoidal rotor current (*Target I*) [11][12], or symmetrical sinusoidal stator current (*Target II*) [14] are not discussible, they can be quite easily obtained independently of the occurring harmonics and asymmetry in the grid voltage by adequate filtration of the reference stator current or rotor current vector components [13], with no need for harmonics and negative sequence separate control. However, these targets introduce a high amount of electromagnetic torque oscillations and for some kind of electromechanical systems with gear-boxes (such as, e.g., wind turbines) should not be implemented.

In *Target IV*, the authors of [9] propose elimination of q_s stator power component oscillations produced by both imbalance and harmonics. Although the presented analysis is accurate and the simulation and experimental results confirm the presented theory, it can be extended by additional targets not considered in the publication, also producing electromagnetic torque oscillations cancellation, but with better quality of the stator current. The first new target is reduction of electromagnetic torque oscillations created by the negative sequence only with sinusoidal unbalanced stator current (relatively small torque oscillations made by harmonics are not eliminated – *Target V*). The second new target is torque oscillations cancellation with a minimum amount of harmonics in the stator current *(Target VI)*.

Electromagnetic torque oscillations during grid voltage imbalance and harmonics are created mainly by the mutual influence of negative sequence flux and positive sequence current, and positive sequence flux and negative sequence current. Even a slight imbalance of grid voltage influences the torque waveform and introduces significant oscillations when

Manuscript received ………………….; revised ……………………; accepted …………………….

The work was supported by the National Science Centre within the project granted on the basis of the decision number 2016/23/B/ST7/03942.

The authors are with the Institute of Control and Industrial Electronics, Warsaw University of Technology, Warszawa, 00-662, Poland (corresponding author e-mail: iwanskig@isep.pw.edu.pl).

1949-3029 (c) 2019 IEEE. Personal use is permitted, but republication/redistribution requires IEEE permission. See http://www.ieee.org/publications_standards/publications/rights/index.html for more information.

This article has been accepted for publication in a future issue of this journal, but has not been fully edited. Content may change prior to final publication. Citation information: DOI 10.1109/TSTE.2019.2935156, IEEE Transactions on Sustainable Energy

adequate control reducing torque oscillations is not applied. *Target V* is obtained by consideration of the negative sequence current component which impacts torque oscillations, and neglecting the current harmonics not to generate harmonics to the grid. This way the control method can be significantly simplified, whereas torque oscillations are not significant [10][13].

The influence of grid voltage harmonics on the electromagnetic torque is weaker than the influence of negative sequence, because the content of harmonic in stator flux is k-times smaller than in grid voltage, where k is the grid voltage harmonic order. Taking it into consideration, it can be proved that e.g., 10% of voltage negative sequence has more significant influence on the electromagnetic torque than 10% of 5th or 7th harmonic of the grid voltage.

This paper focuses on inner control of a doubly fed induction machine connected to the unbalanced and distorted grid. The main goal is to show that more than one target is possible, which provides electromagnetic torque oscillations cancellation of DFIG. *Target IV* (electromagnetic torque oscillations cancellation with a constant q_s component of power) is not necessarily the best option in terms of stator current quality. The paper shows theoretical analysis of other targets, and discussion on practical implementation, taking into consideration that grid voltage may contain not only low order harmonics, which can easily be controlled by proportional-resonant controllers, but also higher order harmonics closer to the sampling and switching frequency, for which control is difficult due to the limitation of resonant terms of rotor current controllers.

II. Influence of Voltage Imbalance and Harmonics on Electromagnetic Torque Oscillations

A. Model of Doubly Fed Induction Machine

The equations of a doubly fed induction machine model of electric circuit in stationary coordinates are (1)-(4)

$$u_s = R_s i_s + \frac{d\psi_s}{dt} \tag{1}$$

$$u_r = R_r i_r + \frac{d\psi_r}{dt} - j\omega_m \psi_r \tag{2}$$

$$\psi_s = L_s i_s + L_m i_r \tag{3}$$

$$\psi_r = L_r i_r + L_m i_s \tag{4}$$

in which u_s, u_r are the vectors of stator and rotor voltage; ψ_s, ψ_r are the vectors of stator and rotor flux; i_s, i_r, are the vectors of stator and rotor current, R_s, R_r are stator and rotor resistances, L_s, L_r, L_m are stator, rotor and magnetizing inductance; ω_m is rotor speed scaled by the number of poles pairs.

Stator flux can be calculated by (5).

$$\psi_s = \int (u_s - R_s i_s)\, dt \tag{5}$$

In practice it is made by low pass filters, which eliminate offsets of sensors and integrator initial state.

One of the possible torque equations using stator flux and stator current vector components in a stationary $\alpha\beta$ frame equals (6), where p_p is the number of poles pairs, whereas the q_s component of instantaneous stator power equals (7).

$$T_{em} = \frac{3}{2} p_p \left(\psi_{s\alpha} i_{s\beta} - \psi_{s\beta} i_{s\alpha}\right) \tag{6}$$

$$q_s = \frac{3}{2}\left(u_{s\beta} i_{s\alpha} - u_{s\alpha} i_{s\beta}\right) \tag{7}$$

Assuming that steady state stator voltage contains fundamental positive and negative sequence components, and additionally is distorted by most commonly existing *5th* negative sequence, and *7th* positive sequence harmonics, voltage waveforms are described by (8)(9)

$$u_{s\alpha} = |u_{sp}| cos(\omega_s t + \varphi_{usp}) + |u_{sn}| sin(\omega_s t + \varphi_{usn}) + |u_{s5}| sin(5\omega_s t + \varphi_{us5}) + |u_{s7}| cos(7\omega_s t + \varphi_{us7}) \tag{8}$$

$$u_{s\beta} = |u_{sp}| sin(\omega_s t + \varphi_{usp}) + |u_{sn}| cos(\omega_s t + \varphi_{usn}) + |u_{s5}| cos(5\omega_s t + \varphi_{us5}) + |u_{s7}| sin(7\omega_s t + \varphi_{us7}) \tag{9}$$

where ω_s is the stator voltage fundamental harmonics pulsation and indexes p, n, 5, and 7 are related to the positive and negative sequences, and fifth and seventh harmonics respectively. Stator flux components as the derivatives of stator voltage vector components are described by (10)(11)

$$\psi_{s\alpha} = \frac{|u_{sp}|}{\omega_s} sin(\omega_s t + \varphi_{usp}) - \frac{|u_{sn}|}{\omega_s} cos(\omega_s t + \varphi_{usn}) - \frac{|u_{s5}|}{5\omega_s} cos(5\omega_s t + \varphi_{us5}) + \frac{|u_{s7}|}{7\omega_s} sin(7\omega_s t + \varphi_{us7}) \tag{10}$$

$$\psi_{s\beta} = -\frac{|u_{sp}|}{\omega_s} cos(\omega_s t + \varphi_{usp}) + \frac{|u_{sn}|}{\omega_s} sin(\omega_s t + \varphi_{usn}) + \frac{|u_{s5}|}{5\omega_s} sin(5\omega_s t + \varphi_{us5}) - \frac{|u_{s7}|}{7\omega_s} cos(7\omega_s t + \varphi_{us7}) \tag{11}$$

For the case in which the stator current contains only positive and negative sequence of fundamental frequency, and 5th and 7th harmonics that are the components occurring in grid voltage (12)(13)

$$i_{s\alpha} = |i_{sp}| cos(\omega_s t + \varphi_{isp}) + |i_{sn}| sin(\omega_s t + \varphi_{isn}) + |i_{s5}| sin(5\omega_s t + \varphi_{is5}) + |i_{s7}| cos(7\omega_s t + \varphi_{is7}) \tag{12}$$

$$i_{s\beta} = |i_{sp}| sin(\omega_s t + \varphi_{isp}) + |i_{sn}| cos(\omega_s t + \varphi_{isn}) + |i_{s5}| cos(5\omega_s t + \varphi_{is5}) + |i_{s7}| sin(7\omega_s t + \varphi_{is7}) \tag{13}$$

electromagnetic torque based on (6), with consideration of (10)-(13) can be derived as (14).

The torque waveform contains a constant component T_{em_const} (15) and an oscillatory component T_{em_osc} (16) represented by 2nd, 4th, 6th, 8th, and 12th harmonic, of which 2nd and 6th are dominating, and 4th, 8th and 12th are at a negligible level, taking into consideration that negative sequence for a doubly fed induction machine proper operation in the steady state cannot be higher than 15-20% [15] in most favorable conditions (synchronous speed operation).

Based on (16), conditions (17) can be assigned for negative sequence and harmonics components to eliminate dominating electromagnetic torque oscillations when both types of disturbances (negative sequence and imbalance) of grid voltage occur, assuming that only fundamental positive and negative sequence, and 5th and 7th harmonics in the stator current are allowed.

1949-3029 (c) 2019 IEEE. Personal use is permitted, but republication/redistribution requires IEEE permission. See http://www.ieee.org/publications_standards/publications/rights/index.html for more information.

$$T_{em}=\frac{3}{2}p_p\left(\left(\frac{|u_{sp}|}{\omega_s}sin(\omega_s t+\varphi_{usp})-\frac{|u_{sn}|}{\omega_s}cos(\omega_s t+\varphi_{usn})-\frac{|u_{s5}|}{5\omega_s}cos(5\omega_s t+\varphi_{us5})+\frac{|u_{s7}|}{7\omega_s}sin(7\omega_s t+\varphi_{us7})\right)\right.$$
$$\left(|i_{sp}|sin(\omega_s t+\varphi_{isp})+|i_{sn}|cos(\omega_s t+\varphi_{isn})+|i_{s5}|cos(5\omega_s t+\varphi_{is5})+|i_{s7}|sin(7\omega_s t+\varphi_{is7})\right)$$
$$-\left(-\frac{|u_{sp}|}{\omega_s}cos(\omega_s t+\varphi_{usp})+\frac{|u_{sn}|}{\omega_s}sin(\omega_s t+\varphi_{usn})+\frac{|u_{s5}|}{5\omega_s}sin(5\omega_s t+\varphi_{us5})-\frac{|u_{s7}|}{7\omega_s}cos(7\omega_s t+\varphi_{us7})\right)$$
$$\left(|i_{sp}|cos(\omega_s t+\varphi_{isp})+|i_{sn}|sin(\omega_s t+\varphi_{isn})+|i_{s5}|sin(5\omega_s t+\varphi_{is5})+|i_{s7}|cos(7\omega_s t+\varphi_{is7})\right)=$$
$$\frac{3}{2}p_p\left(\frac{|u_{sp}||i_{sp}|}{\omega_s}cos(\varphi_{usp}-\varphi_{isp})+\frac{|u_{sp}||i_{sn}|}{\omega_s}sin(2\omega_s t+\varphi_{usp}+\varphi_{isn})+\frac{|u_{sp}||i_{s5}|}{\omega_s}sin(6\omega_s t+\varphi_{usp}+\varphi_{is5})\right.$$
$$+\frac{|u_{sp}||i_{s7}|}{\omega_s}cos(-6\omega_s t+\varphi_{usp}-\varphi_{is7})-\frac{|u_{sn}||i_{sp}|}{\omega_s}sin(2\omega_s t+\varphi_{usn}+\varphi_{isp})-\frac{|u_{sn}||i_{sn}|}{\omega_s}cos(\varphi_{usn}-\varphi_{isn})$$
$$-\frac{|u_{sn}||i_{s5}|}{\omega_s}cos(-4\omega_s t+\varphi_{usn}-\varphi_{is5})-\frac{|u_{sn}||i_{s7}|}{\omega_s}sin(8\omega_s t+\varphi_{usn}+\varphi_{is7})-\frac{|u_{s5}||i_{sp}|}{5\omega_s}sin(6\omega_s t+\varphi_{us5}+\varphi_{isp})$$
$$-\frac{|u_{s5}||i_{sn}|}{5\omega_s}cos(4\omega_s t+\varphi_{us5}-\varphi_{isn})-\frac{|u_{s5}||i_{s5}|}{5\omega_s}cos(\varphi_{us5}-\varphi_{is5})-\frac{|u_{s5}||i_{s7}|}{5\omega_s}sin(12\omega_s t+\varphi_{us5}+\varphi_{is7})$$
$$+\frac{|u_{s7}||i_{sp}|}{7\omega_s}cos(6\omega_s t+\varphi_{us7}-\varphi_{isp})+\frac{|u_{s7}||i_{sn}|}{7\omega_s}sin(8\omega_s t+\varphi_{us7}+\varphi_{isn})+\frac{|u_{s7}||i_{s5}|}{7\omega_s}sin(12\omega_s t+\varphi_{us7}+\varphi_{is5})$$
$$\left.+\frac{|u_{s7}||i_{s7}|}{7\omega_s}cos(\varphi_{us7}-\varphi_{is7})\right) \tag{14}$$

$$T_{em\_const}=\frac{3}{2}p_p\left(\frac{|u_{sp}||i_{sp}|}{\omega_s}cos(\varphi_{usp}-\varphi_{isp})-\frac{|u_{sn}||i_{sn}|}{\omega_s}cos(\varphi_{usn}-\varphi_{isn})-\frac{|u_{s5}||i_{s5}|}{5\omega_s}cos(\varphi_{us5}-\varphi_{is5})+\frac{|u_{s7}||i_{s7}|}{7\omega_s}cos(\varphi_{us7}-\varphi_{is7})\right) \tag{15}$$

$$T_{em\_osc}=\frac{3}{2}p_p\left(\frac{|u_{sp}||i_{sn}|}{\omega_s}sin(2\omega_s t+\varphi_{usp}+\varphi_{isn})+\frac{|u_{sp}||i_{s5}|}{\omega_s}sin(6\omega_s t+\varphi_{usp}+\varphi_{is5})+\frac{|u_{sp}||i_{s7}|}{\omega_s}cos(-6\omega_s t+\varphi_{usp}-\varphi_{is7})-\right.$$
$$\frac{|u_{sn}||i_{sp}|}{\omega_s}sin(2\omega_s t+\varphi_{usn}+\varphi_{isp})-\frac{|u_{sn}||i_{s5}|}{\omega_s}cos(-4\omega_s t+\varphi_{usn}-\varphi_{is5})-\frac{|u_{sn}||i_{s7}|}{\omega_s}sin(8\omega_s t+\varphi_{usn}+\varphi_{is7})-$$
$$\frac{|u_{s5}||i_{sp}|}{5\omega_s}sin(6\omega_s t+\varphi_{us5}+\varphi_{isp})-\frac{|u_{s5}||i_{sn}|}{5\omega_s}cos(4\omega_s t+\varphi_{us5}-\varphi_{isn})-\frac{|u_{s5}||i_{s7}|}{5\omega_s}sin(12\omega_s t+\varphi_{us5}+\varphi_{is7})+$$
$$\left.\frac{|u_{s7}||i_{sp}|}{7\omega_s}cos(6\omega_s t+\varphi_{us7}-\varphi_{isp})+\frac{|u_{s7}||i_{sn}|}{7\omega_s}sin(8\omega_s t+\varphi_{us7}+\varphi_{isn})+\frac{|u_{s7}||i_{s5}|}{7\omega_s}sin(12\omega_s t+\varphi_{us7}+\varphi_{is5})\right) \tag{16}$$

This way the conditions (17) allow us to eliminate the most significant torque oscillation made by mutual reaction of positive sequence flux component and negative sequence, 5th and 7th harmonics of the stator current vector, as well as positive sequence current and negative sequence, 5th and 7th harmonics of the stator flux.

$$\begin{cases}|i_{sn}|=\frac{|u_{sn}|}{|u_{sp}|}|i_{sp}|;\ \varphi_{isn}=-\varphi_{usp}+\varphi_{usn}+\varphi_{isp}\\ |i_{s5}|=\frac{|u_{s5}|}{5|u_{sp}|}|i_{sp}|;\ \varphi_{is5}=-\varphi_{usp}+\varphi_{us5}+\varphi_{isp}\\ |i_{s7}|=-\frac{|u_{s7}|}{7|u_{sp}|}|i_{sp}|;\ \varphi_{is7}=\varphi_{usp}+\varphi_{us7}-\varphi_{isp}\end{cases} \tag{17}$$

Conditions (17) do not coincide with conditions (18) necessary to eliminate 4th, 8th, and 12th harmonics oscillations in the torque made by the reaction of negative sequence, 5th and 7th harmonics of the stator flux with negative sequence, 5th and 7th harmonics of the stator current.

$$\begin{cases}|i_{s5}|=-\frac{|u_{s5}|}{5|u_{sn}|}|i_{sn}|;\ \varphi_{is5}=\varphi_{usn}+\varphi_{us5}-\varphi_{isn}\\ |i_{s7}|=\frac{|u_{s7}|}{7|u_{sn}|}|i_{sn}|;\ \varphi_{is7}=-\varphi_{usn}+\varphi_{us7}+\varphi_{isn}\\ |i_{s5}|=\frac{7|u_{s5}|}{5|u_{s7}|}|i_{s7}|;\ \varphi_{is5}=-\varphi_{us7}+\varphi_{us5}+\varphi_{is7}\end{cases} \tag{18}$$

However, the influence of mutual interactions between negative sequence flux and current harmonics components, as well as negative sequence current and harmonics flux components on torque oscillations is at a negligible level, especially in the case of a relatively small amount of negative sequence stator voltage (so flux) allowing safe operation of the

1949-3029 (c) 2019 IEEE. Personal use is permitted, but republication/redistribution requires IEEE permission. See http://www.ieee.org/publications_standards/publications/rights/index.html for more information.

doubly fed induction machine. Totally negligible are the mutual interactions of 5^{th} and 7^{th} harmonic of stator flux with 5^{th} and 7^{th} harmonic of the stator current due to 5 and 7 times lower amount of 5^{th} and 7^{th} harmonics in the flux than in the stator voltage respectively.

III. Reference Stator Current Calculation for Non-Oscillating Torque Conditions

In this section, three targets will be presented. *Target V* and *Target VI* not considered in earlier publications will be compared to the basic target providing torque oscillations cancellation with a constant q_s component of instantaneous power presented in [9] (*Target IV*). Ideal cases mean that the stator current harmonics are fully controlled and obtained at a reference value without steady state error for the harmonics orders which occur in the grid voltage (5^{th} harmonic negative sequence and 7^{th} harmonic positive sequence). For these harmonics resonant terms are applied in a rotor current vector control. Parameters of the 2MW doubly fed induction machine are presented in Table I.

TABLE I
Parameters of a 2MW DFIG from simulation tests

Symbol	Parameter	Value
P_n	Rated power	2MW
U_{sn}	Stator rated voltage (Y)	690V
I_{sn}	Rated stator current (Y)	1760A
U_{rn}	Stator/rotor turns ratio	0.34
R_s	Stator resistance	26mΩ
L_s	Stator leakage inductance	0.087mH
R_r	Rotor resistance	26mΩ
L_r	Rotor leakage inductance	0.087mH
L_m	Magnetizing inductance	2.5mH
p_p	Number of poles pairs	2

A. *Target IV – constant q_s component of stator power*

Vector control requires two orthogonal components of current vector as reference signals. These components can be calculated on the basis of the reference torque and another reference variable, which can be alternatively rotor flux vector length depending on the desired q_s component of instantaneous power [16] or directly the q_s component of instantaneous power [17]. The reference rotor flux vector length can be calculated for the symmetrical sinusoidal grid voltage [18], but such a way of reference flux length determination introduces strong harmonics in the stator current at unbalanced and/or distorted grid voltage operation. Definitely, the reference rotor flux cannot be set constant like in [19], but it must be matched to the varying stator flux during grid voltage imbalance and harmonics to achieve not only constant torque but also satisfactory shape of the stator current.

Direct use of instantaneous power q_s component instead of rotor flux vector length for reference current calculation is possible. Using torque T_{em} and q_s component power equations (6)(7), the reference stator current vector components can be derived (19)(20), replacing the torque T_{em} and q_s component of power by reference signals T_{em}^{ref} and q_s^{ref} respectively.

$$i_{s\alpha}^{ref} = \frac{2}{3p_p}\frac{p_p q_s^{ref}\psi_{s\alpha}+T_{em}^{ref}u_{s\alpha}}{u_{s\beta}\psi_{s\alpha}-u_{s\alpha}\psi_{s\beta}} \tag{19}$$

$$i_{s\beta}^{ref} = \frac{2}{3p_p}\frac{p_p q_s^{ref}\psi_{s\beta}+T_{em}^{ref}u_{s\beta}}{u_{s\beta}\psi_{s\alpha}-u_{s\alpha}\psi_{s\beta}} \tag{20}$$

The use of the constant reference component of power q_s^{ref} introduces some amount of harmonics in the stator current when grid voltage is distorted, but torque oscillations are insignificant. For a small amount of harmonics, this target provides a negligible level of stator current harmonics [20]. Stator phase current waveforms and rotor phase current waveforms for constant torque T_{em} and constant q_s component of stator power when negative sequence and 5^{th} and 7^{th} harmonics in the grid voltage occur, are shown in Fig. 1.

B. *Target V – sinusoidal unbalanced stator current*

[10] proposes a way to obtain sinusoidal stator current for several targets without sequences decomposition when unbalanced grid voltage operation of DFIG is taken into account. The harmonics were treated as a disturbance not influencing electromagnetic torque pulsations strongly. One of the presented targets (*Target V*) gives sinusoidal unbalanced stator current eliminating torque oscillations due to the negative sequence occurrence. Not to implement a negative sequence extraction structure, the constant q_s component of stator power has been referenced, but for calculation of reference stator current vector components, both stator flux and grid voltage have been filtered to obtain only 50Hz components of these variables (21)(22).

$$i_{s\alpha}^{ref} = \frac{2}{3p_p}\frac{p_p q_s^{ref}\psi_{s\alpha1}+T_{em}^{ref}u_{s\alpha1}}{u_{s\beta1}\psi_{s\alpha1}-u_{s\alpha1}\psi_{s\beta1}} \tag{21}$$

$$i_{s\beta}^{ref} = \frac{2}{3p_p}\frac{p_p q_s^{ref}\psi_{s\beta1}+T_{em}^{ref}u_{s\beta1}}{u_{s\beta1}\psi_{s\alpha1}-u_{s\alpha1}\psi_{s\beta1}} \tag{22}$$

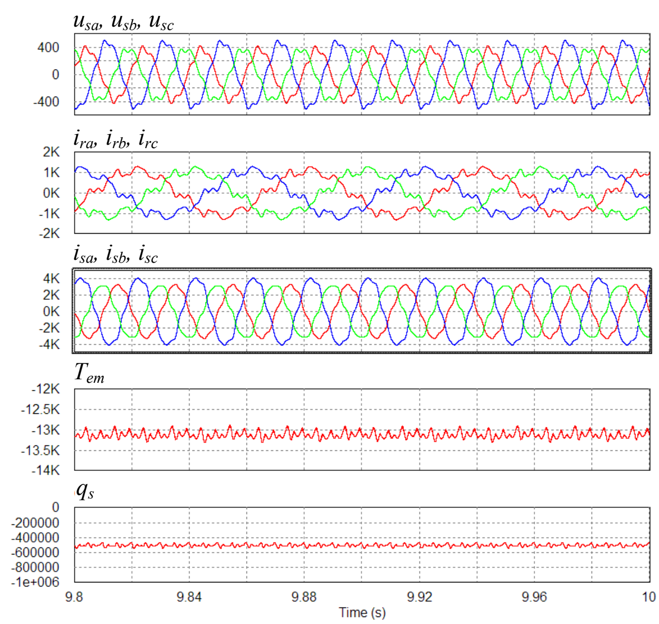

Fig. 1. Stator phase voltage u_{sa}, u_{sb}, u_{sc}, rotor phase current i_{ra}, i_{rb}, i_{rc}, stator phase current i_{sa}, i_{sb}, i_{sc}, electromagnetic torque T_{em}, and real q_s component of instantaneous stator power for constant reference torque and constant reference q_s component of power (*Target IV*) at stator voltage distorted by low frequencies.

1949-3029 (c) 2019 IEEE. Personal use is permitted, but republication/redistribution requires IEEE permission. See http://www.ieee.org/publications_standards/publications/rights/index.html for more information.

This article has been accepted for publication in a future issue of this journal, but has not been fully edited. Content may change prior to final publication. Citation information: DOI 10.1109/TSTE.2019.2935156, IEEE Transactions on Sustainable Energy

Fig. 2 presents reference current waveforms calculated using (21)(22), and the true waveform of electromagnetic torque. It can be seen that electromagnetic torque oscillations contain mainly 300Hz components. They are insignificant for the assumed 8% THD factor of grid voltage (5.5%).

C. Target VI – torque oscillations cancellation with a minimum amount of harmonics

For distorted grid voltage, the way of calculation of this reference signal can be modified, and thus the control in some way extended. To meet the set of conditions (17), it is required to determine the required oscillating component in the q_s component of power and set them in the reference signal q_s^{ref} when using (19)(20). It requires sequences decomposition and harmonics extraction. Another way to achieve this condition is to set q_s^{ref} constant and introduce compensation terms, or set the reference current negative sequence and harmonics components directly based on the conditions (17). This way we have parallel control paths and, what is more troublesome, introduce many parallel structures responsible for symmetrical sequences decomposition and harmonics extraction [21].

The simplest way is to use a new variable z_s introduced with consideration of all conditions (17) related to negative sequence and harmonics. Variable z_s is described by (23).

$$z_s = \frac{3}{2}\left(\left(u_{s\beta 1} + \frac{u_{s\beta 5}}{5} - \frac{u_{s\beta 7}}{7}\right) i_{s\alpha} - \left(u_{s\alpha 1} + \frac{u_{s\alpha 5}}{5} - \frac{u_{s\alpha 7}}{7}\right) i_{s\beta}\right) = \frac{3}{2}\left(u'_{s\beta} i_{s\alpha} - u'_{s\alpha} i_{s\beta}\right) \tag{23}$$

Calculated this way, the new variable meeting conditions (17) contains hardly any oscillations. Moreover, its average value with negligible error equals the average value of the q_s component of instantaneous power. Due to the fact that this variable is constant, it is a good signal for reference when both negative sequence and grid voltage harmonics occur.

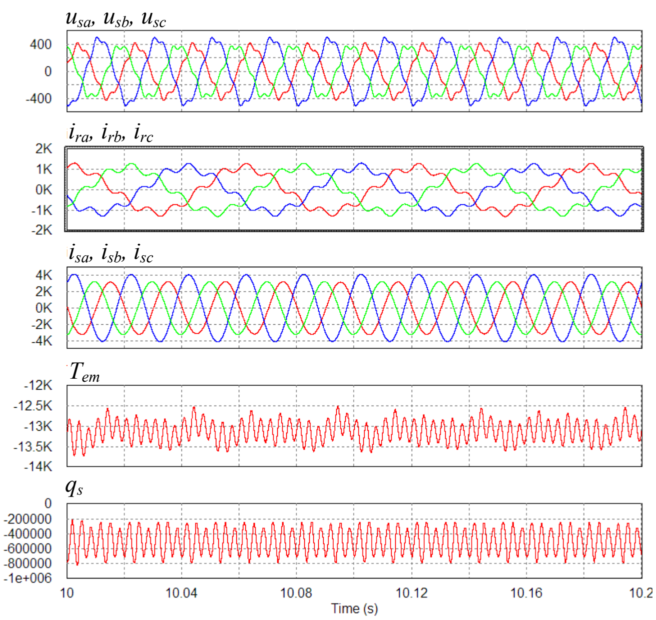

Fig. 2. Stator phase voltage u_{sa}, u_{sb}, u_{sc}, rotor phase current i_{ra}, i_{rb}, i_{rc}, stator phase current i_{sa}, i_{sb}, i_{sc}, electromagnetic torque T_{em}, and real q_s component of instantaneous stator power for constant reference torque and sinusoidal unbalanced stator current (*Target V*) at stator voltage distorted by low frequencies.

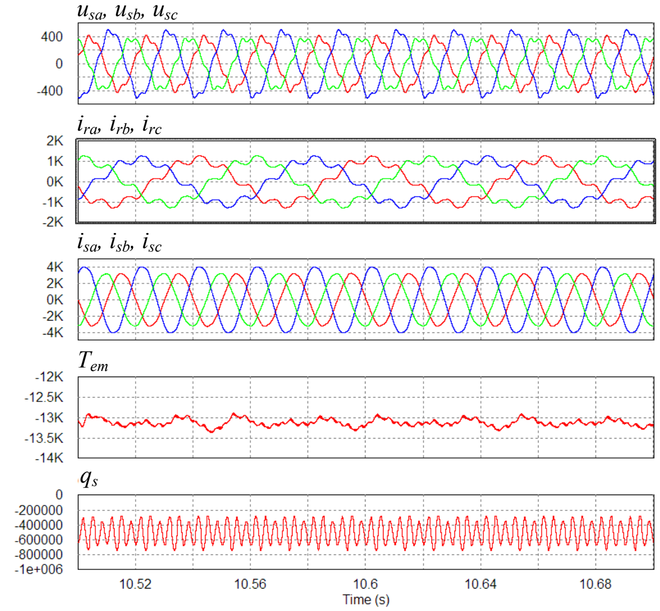

Fig. 3. Stator phase voltage u_{sa}, u_{sb}, u_{sc}, rotor phase current i_{ra}, i_{rb}, i_{rc}, stator phase current i_{sa}, i_{sb}, i_{sc}, electromagnetic torque T_{em}, and real q_s component of instantaneous stator power for constant reference torque and minimum harmonics in the stator current (*Target VI*) at stator voltage distorted by low frequencies.

Using this new reference value z_s^{ref}, the reference stator current vector components $i_{s\alpha}^{ref}, i_{s\beta}^{ref}$ can be assigned (24)(25).

$$i_{s\alpha}^{ref} = \frac{2}{3p_p} \frac{p_p z_s^{ref} \psi_{s\alpha} + T_{em}^{ref} u'_{s\alpha}}{u'_{s\beta}\psi_{s\alpha} - u'_{s\alpha}\psi_{s\beta}} \tag{24}$$

$$i_{s\beta}^{ref} = \frac{2}{3p_p} \frac{p_p z_s^{ref} \psi_{s\beta} + T_{em}^{ref} u'_{s\beta}}{u'_{s\beta}\psi_{s\alpha} - u'_{s\alpha}\psi_{s\beta}} \tag{25}$$

Calculated this way, the reference stator current contains a small amount of harmonics (Fig. 3), and insignificant torque pulsations due to the fact that only conditions (17) are met, whereas conditions (18) cannot be met using only the harmonics that occur in grid voltage.

D. Multi-band-pass filter for z_s^{ref} calculation in Target VI

The reference z_s^{ref} variable requires a multi-band-pass filter of the stator (grid) voltage. It is obtained by three different band-pass filters (each in a separate band for f_1=50Hz, f_5=250Hz and f_7=350Hz). A general transfer function for each separate filter is written as (26).

$$G(s) = \frac{k_{BPF}(\Delta\omega)s}{s^2 + (\Delta\omega)s + \omega_0^2} \tag{26}$$

where k_{BPF} is filter gain for resonant frequency, $\Delta\omega$ is filter band, ω_o is resonant frequency. For each filter, gains are assumed $k_{BPF1} = 1$ for 50Hz, $k_{BPF5} = 1/5$ for 250Hz, and $k_{BPF7} = -1/7$ for 350Hz, and filters bands $\Delta f_1 = 1.25Hz, \Delta f_5 = 6.25Hz, \Delta f_7 = 8.75Hz$ respectively, taking into consideration that typically the fundamental frequency may change in the range $\pm 0.5Hz$.

A digital representation of the transfer function can be obtained with the Tustin discretization method with pre-warping to eliminate shift of discrete filter resonant frequency in relation to continuous filter resonant frequency. The obtained transfer functions for each band pass filter are:

1949-3029 (c) 2019 IEEE. Personal use is permitted, but republication/redistribution requires IEEE permission. See http://www.ieee.org/publications_standards/publications/rights/index.html for more information.

This article has been accepted for publication in a future issue of this journal, but has not been fully edited. Content may change prior to final publication. Citation information: DOI 10.1109/TSTE.2019.2935156, IEEE Transactions on Sustainable Energy

$$G_1(z) = \frac{0.0009797777906047484(z^2-1)}{z^2-1.991881152540935z+0.99804044448791} \quad (27a)$$

$$G_5(z) = \frac{0.0009521539118237673(z^2-1)}{z^2-1.838962309913228z+0.990478460881763} \quad (27b)$$

$$G_7(z) = -\frac{0.0009269788373778304(z^2-1)}{z^2-1.694215017272620z+0.987022296276710} \quad (27c)$$

while the total transfer function of the applied multi-band pass filter is described by (28).

$$G_{MBPF}(z) = G_1(z) + G_5(z) + G_7(z) \quad (28)$$

The general property of the applied multi-band-pass filter is that grid voltage harmonics are *k*-times damped, where *k* is the harmonics order, so the amplitude behaves like passed by integral part scaled by pulsation, but the harmonics components phases are not shifted by 90 degrees like during integration (so like in flux calculation) but remain unchanged for fundamental harmonics and all negative sequence components (including negative sequence harmonics such as, e.g., 5^{th}) and is changed to the opposite phase (180 degrees) for positive sequence harmonics (such as 7^{th}). The Bode plots for the applied multi-band-pass filter with comparison to the plots of the integral term gained by fundamental harmonics pulsation are shown in Fig. 4.

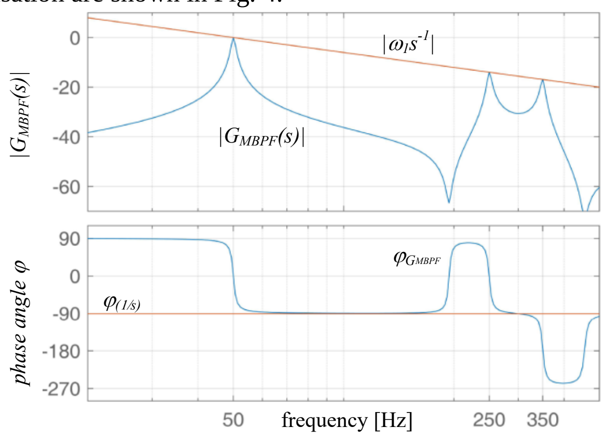

Fig. 4. Bode plots for the applied multi-band-pass filter and for the integral term gained by fundamental harmonics pulsation.

IV. Control Method of DFIG Operating with Unbalanced and Distorted Grid

A scheme of the proposed control of DFIG with rotor current controllers for the analyzed targets is presented in Fig. 5. In the case of a constant q_s stator power component (*Target IV*), a multi-band-pass filter MBPF is not used and instead of filtered $u_{s\alpha\beta}'$ directly measured $u_{s\alpha\beta}$ is used. In the case of sinusoidal unbalanced stator current (*Target V*), stator voltage components $u_{s\alpha\beta}$ are filtered by the band pass filter with 50Hz central frequency to obtain fundamental frequency $\alpha\beta$ components for flux calculation, and MBPF is not used.

To improve the dynamic responses, the control structure is equipped with full feed-forward and decoupling terms. Using (1)-(4), the rotor circuit equation (29) can be obtained

$$u_r = R_r i_r + \sigma L_r \frac{di_r}{dt} + \frac{L_m}{L_s}(u_s - R_s i_s) - j\omega_m(L_r i_r + L_m i_s) \quad (29)$$

in which σ is the leakage factor.

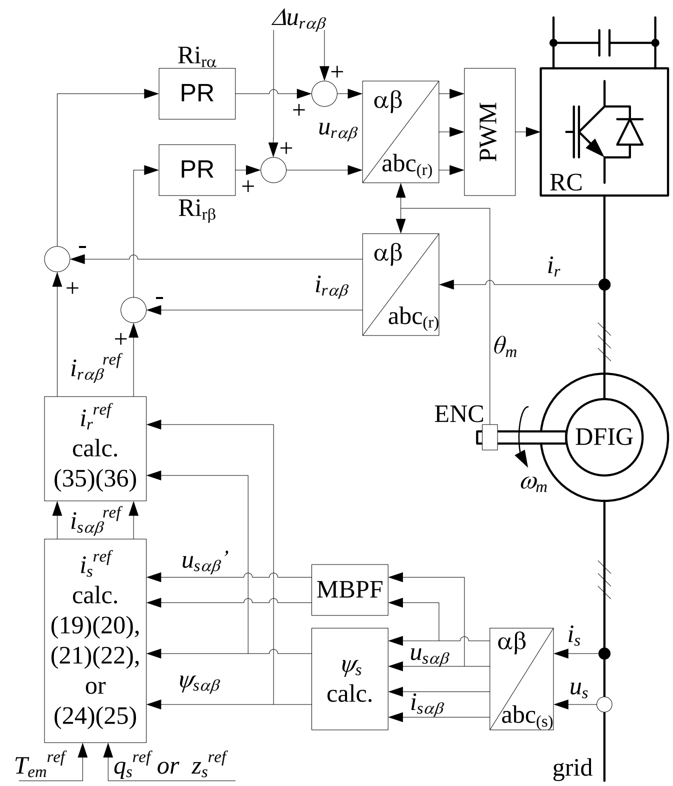

Fig. 5. Scheme of the proposed rotor current vector control of a doubly fed induction machine working with unbalanced and distorted grid voltage.

Terms (30)(31) are decoupling and feed-forward for the control paths with proportional-resonant rotor current components in the stationary $\alpha\beta$ frame.

$$\Delta u_{r\alpha} = \frac{L_m}{L_s}(u_{s\alpha} - R_s i_{s\alpha}) + \omega_m(L_r i_{r\beta} + L_m i_{s\beta}) \quad (30)$$

$$\Delta u_{r\beta} = \frac{L_m}{L_s}(u_{s\beta} - R_s i_{s\beta}) - \omega_m(L_r i_{r\alpha} + L_m i_{s\alpha}) \quad (31)$$

Reference rotor current calculation requires determination of magnetizing current under unbalanced and distorted grid voltage conditions. Magnetizing current vector components in the stationary frame are calculated by (32) and (33).

$$i_{m\alpha} = \frac{\psi_{s\alpha} - L_{\sigma s} i_{s\alpha}^{ref}}{L_m} \quad (32)$$

$$i_{m\beta} = \frac{\psi_{s\beta} - L_{\sigma s} i_{s\beta}^{ref}}{L_m} \quad (33)$$

in which $L_{\sigma s}$ is stator leakage inductance and L_m is magnetizing inductance. According to (34),

$$i_r^{ref} = i_m - i_s^{ref} \quad (34)$$

reference rotor current components are described by (35)(36).

$$i_{r\alpha}^{ref} = \frac{\psi_{s\alpha} - L_s i_{s\alpha}^{ref}}{L_m} \quad (35)$$

$$i_{r\beta}^{ref} = \frac{\psi_{s\alpha} - L_s i_{s\beta}^{ref}}{L_m} \quad (36)$$

1949-3029 (c) 2019 IEEE. Personal use is permitted, but republication/redistribution requires IEEE permission. See http://www.ieee.org/publications_standards/publications/rights/index.html for more information.

This article has been accepted for publication in a future issue of this journal, but has not been fully edited. Content may change prior to final publication. Citation information: DOI 10.1109/TSTE.2019.2935156, IEEE Transactions on Sustainable Energy

V. Simulation Results for the 2MW Machine Model

Simulation tests presented in Section III are an ideal situations, in which it is assumed that the actual stator current is achieved at the reference value (steady state error cancellation) due to the implementation of oscillatory terms in rotor current controllers selected for the frequencies adequate to the grid voltage harmonics disturbance. However, the used classic linear PR controllers have some limitations in control error elimination for higher frequencies. This is why for the grid voltage distorted by higher harmonics close to the switching/sampling frequency it is impossible to obtain stator and rotor currents precisely matching the reference values, when the reference current vector components include higher harmonics close to the sampling frequency or when the control disturbance (grid voltage) contains higher frequency harmonics. This can be observed in the following figures presenting simulation results for the 2MW machine model for different targets. The high frequency disturbance in the grid voltage was obtained by overloading the grid using a three-phase six-pulse diode rectifier.

Fig. 6 presents simulation results for *Target IV*, which is torque oscillations cancellation at a constant q_s component of stator power. The content of torque oscillations is significantly higher than those from Fig. 1. This is because higher frequencies of reference current close to the switching and sampling frequency cannot be properly reproduced in the actual currents by PR regulators to obtain fully non-oscillatory torque and non-oscillatory q_s component of stator instantaneous power.

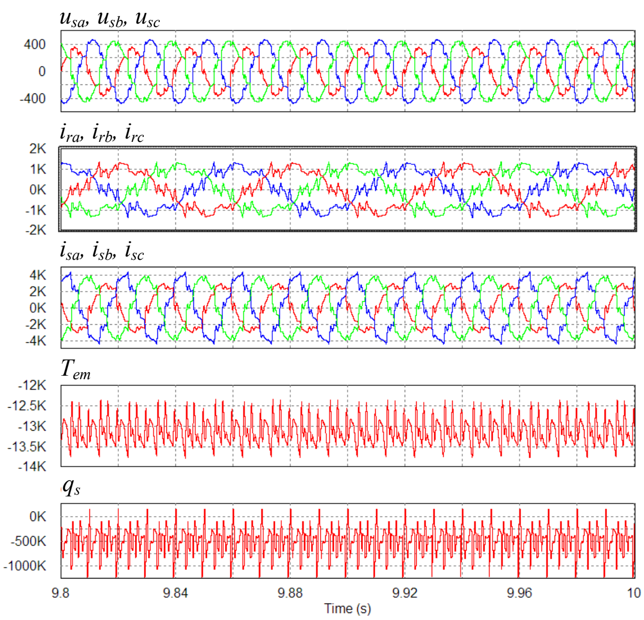

Fig. 6. Stator phase voltage u_{sa}, u_{sb}, u_{sc}, rotor phase current i_{ra}, i_{rb}, i_{rc}, stator phase current i_{sa}, i_{sb}, i_{sc}, electromagnetic torque T_{em}, and real q_s component of instantaneous stator power for constant reference torque and constant reference q_s component of power (*Target IV*) at stator voltage distorted by high frequencies.

Fig. 7 and Fig. 8 present the simulation results of a high power machine operating with strongly distorted grid for sinusoidal unbalanced stator current target and for minimum stator current harmonics content target. In the second case, the torque oscillations are insignificantly smaller, whereas q_s stator power pulsations are the same.

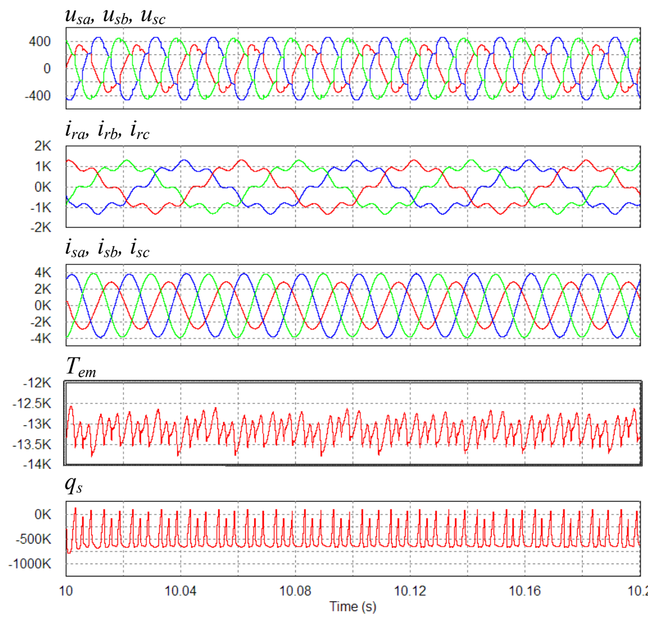

Fig. 7. Stator phase voltage u_{sa}, u_{sb}, u_{sc}, rotor phase current i_{ra}, i_{rb}, i_{rc}, stator phase current i_{sa}, i_{sb}, i_{sc}, electromagnetic torque T_{em}, and real q_s component of instantaneous stator power for constant reference torque and sinusoidal unbalanced stator current (*Target V*) at stator voltage distorted by high frequencies.

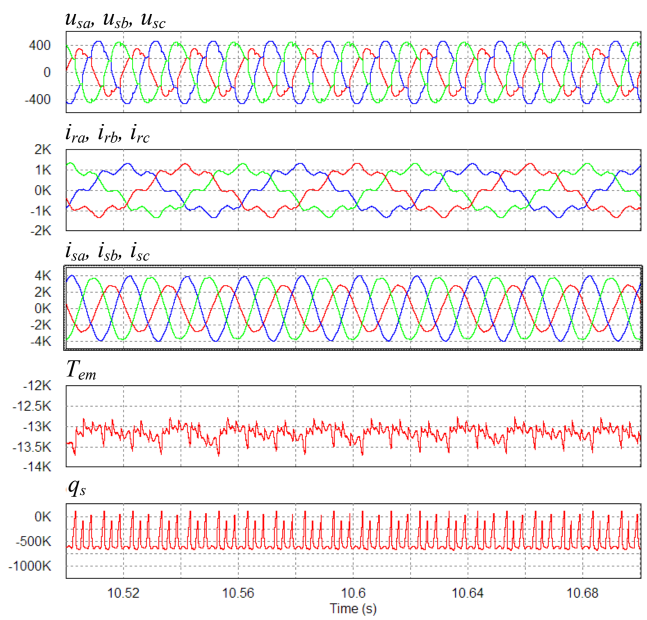

Fig. 8. Stator phase voltage u_{sa}, u_{sb}, u_{sc}, rotor phase current i_{ra}, i_{rb}, i_{rc}, stator phase current i_{sa}, i_{sb}, i_{sc}, electromagnetic torque T_{em}, and real q_s component of instantaneous stator power for constant reference torque and minimum harmonics in the stator current (*Target VI*) at stator voltage distorted by high frequencies.

1949-3029 (c) 2019 IEEE. Personal use is permitted, but republication/redistribution requires IEEE permission. See http://www.ieee.org/publications_standards/publications/rights/index.html for more information.

This article has been accepted for publication in a future issue of this journal, but has not been fully edited. Content may change prior to final publication. Citation information: DOI 10.1109/TSTE.2019.2935156, IEEE Transactions on Sustainable Energy

VI. Experimental Results of the Proposed Control Method under Grid Voltage Imbalance and Harmonics

A. Experimental test rig

Experimental tests for rotor current control were obtained in a laboratory unit with a 7.5kW doubly fed induction machine. The grid side converter GC was controlled using standard voltage oriented control to stabilize DC bus voltage, which is beyond the scope of the paper due to independence of electromagnetic torque oscillations of GC operation. The rotor side converter is controlled with sampling and switching frequency equal to 4kHz.

Parameters of the used doubly fed induction machine are presented in Table II. The machine stator has been connected to the grid in the delta type. Experimental tests have been made with unbalanced and harmonics distorted grid, whereas imbalance has been obtained using a multi-tap transformer and harmonics distortion by a six pulse diode rectifier with large resistive load connected in parallel to the three wire grid.

TABLE II
Parameters of a 7.5 kW DFIG from the Laboratory Unit

Symbol	Parameter	Value
P_n	Rated power	7.5kW
U_{sn}	Stator rated voltage (Δ/Y)	220/380V
I_{sn}	Rated stator current (Δ/Y)	27.4/15.7A
U_{rn}	Rated rotor voltage (0 rpm)	182V
I_{rn}	Rotor rated current	15A
R_s	Stator resistance	0.43Ω
L_s	Stator inductance	130mH
R_r	Rotor resistance	0.71Ω
L_r	Rotor inductance	130mH
L_m	Magnetizing inductance	120mH
n_{mn}	Rated speed	1445rpm
p_p	Number of poles	4

B. Rotor Current Control Experimental Results

Experimental tests have been done for three analyzed cases – constant torque and constant q_s, sinusoidal unbalanced stator current, constant torque with minimum stator current harmonics. However, experiments have been made with a more realistic waveform of grid voltage, which besides dominating 5th and 7th harmonics contains also higher harmonics caused by commutation processes of the three phase six pulse diode rectifier used for the network overload.

Similarly to the cases from section V, the highest torque pulsations are for constant torque and q_s stator power target (Fig. 9). The stator current for this case is far from satisfactory. The cases presenting torque oscillations cancellation with sinusoidal unbalanced stator current (*Target V*) and torque oscillations cancellation with a minimum amount of stator current harmonics (*Target VI*), shown in Fig. 10 and Fig. 11 respectively, are very similar in practice. Oscillations of torque are at the same level, and it is more the influence of measurement noises than the influence of the methods' imperfections. Definitely both cases provide significantly higher quality of stator current delivered to the grid than the current obtained for the typical torque oscillations cancellation target with a constant referenced q_s component of instantaneous stator power (*Target IV*).

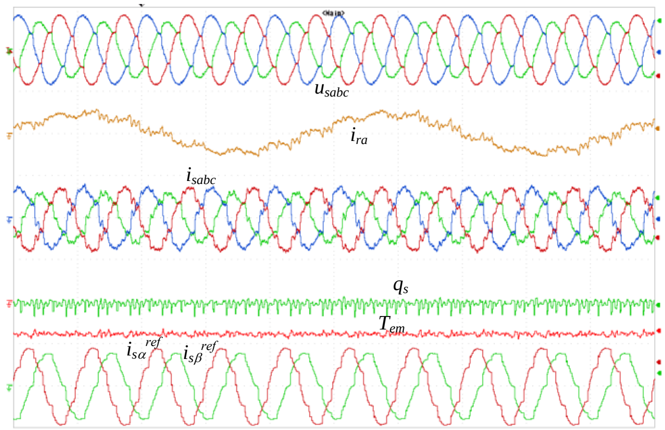

Fig. 9. Laboratory tests results with a small power machine model for grid voltage harmonics obtained using six pulse diode rectifier overload – constant torque and stator q_s power target.

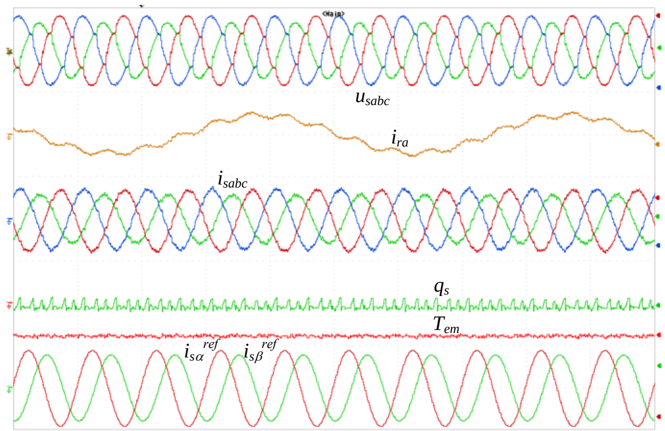

Fig. 10. Laboratory tests results with a small power machine model for grid voltage harmonics obtained using six pulse diode rectifier overload – sinusoidal unbalanced stator current target.

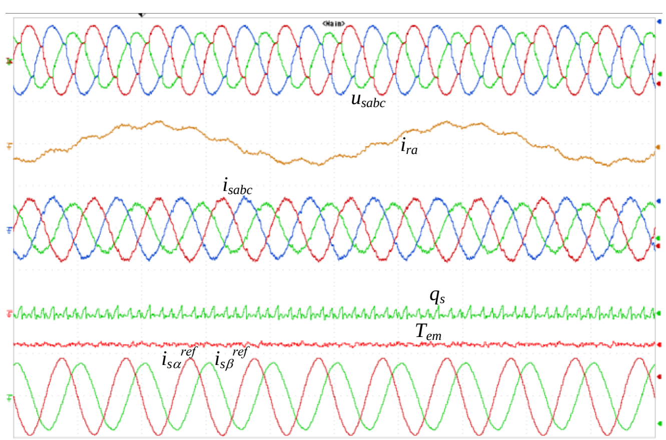

Fig. 11. Laboratory tests results with a small power machine model for grid voltage harmonics obtained using six pulse diode rectifier overload – torque oscillations cancellation with minimum stator current harmonics target.

Fig. 12 presents Fast Fourier Transformation (FFT) spectra for all analyzed targets. As it can be expected, the best shape of stator current has been achieved for the new *Target V* – sinusoidal unbalanced stator current, later for the new *Target VI* – a minimum amount of stator current harmonics giving torque oscillations cancellation, whereas the worst quality of stator current has been obtained for the known *Target IV* – a constant q_s component of stator power.

1949-3029 (c) 2019 IEEE. Personal use is permitted, but republication/redistribution requires IEEE permission. See http://www.ieee.org/publications_standards/publications/rights/index.html for more information.

This article has been accepted for publication in a future issue of this journal, but has not been fully edited. Content may change prior to final publication. Citation information: DOI 10.1109/TSTE.2019.2935156, IEEE Transactions on Sustainable Energy

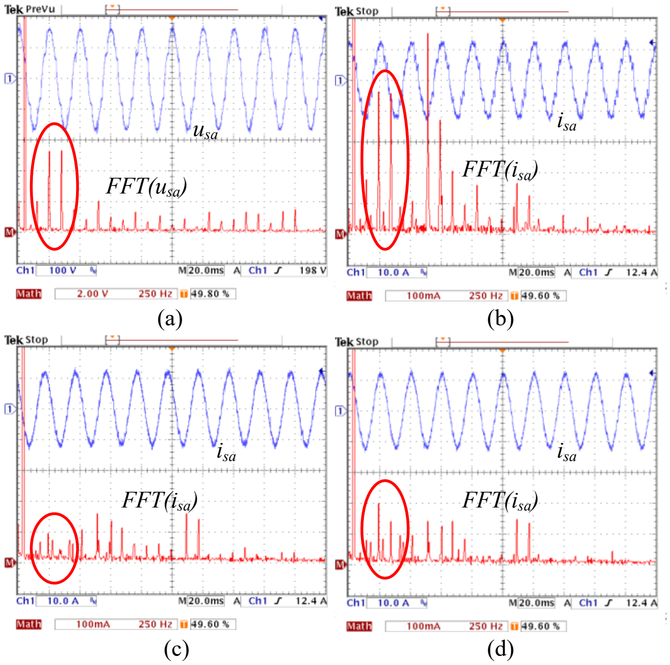

Fig. 12. FFT spectra of a) stator (grid) voltage, and stator current obtained for b) *Target IV* – a constant q_s component of stator power, c) *Target V* – sinusoidal unbalanced stator current and d) *Target VI* – a minimum amount of stator current harmonics giving non oscillatory torque.

Table III presents the THD_i factor of stator current for each target, whereas the THD_u factor of grid voltage is the same for each target and equals 5.5%. According to the newest *IEEE 519-2014 Standard* [22] on voltage and current harmonics in the electric power network, stator current harmonics content in all targets meets requirements for short circuit current I_{SC} to load current I_L ratio higher than 50. For the ratio lower than 50, 13^{th} stator current harmonic in *Target IV*, exceeds the 3.5% limit. For the ratio lower than 20, 13^{th} and 15^{th} harmonics exceeds the 2% limit, whereas 5^{th} and 7^{th} harmonics are close to the 4% limit. *Target V* and *Target VI* meet Standards requirements for the whole range of short circuit current to the load current ratio.

TABLE III
STATOR CURRENT THD FOR EACH TARGET

HARMONIC ORDER/THD	TARGET IV	TARGET V	TARGET VI
3^{rd}	0.16A (1.3%)	0A (0%)	0.06A (0.5%)
$\mathbf{5^{th}}$	**0.46A (3.8%)**	0.08A (0.7%)	0.19A (1.6%)
$\mathbf{7^{th}}$	**0.46A (3.8%)**	0A (0%)	0.13A (1.1%)
9^{th}	0.08A (0.7%)	0.06A (0.5%)	0.09A (0.7%)
11^{th}	0.1A (0.8%)	0.1A (0.8%)	0.09A (0.7%)
$\mathbf{13^{th}}$	**0.64A (5%)**	0.15A (1.2%)	0.13A (1.1%)
$\mathbf{15^{th}}$	**0.36A (3%)**	0.13A (1.1%)	0.12A (1%)
17^{th}	0.2A (1.7%)	0.1A (0.8%)	0.13A (1.1%)
$THD_{\%}$	8.8	2.8	3.4

Fig. 13 presents simulation results of a small scale machine model. Similar results to those obtained in the experimental tests substantiate the simulation results of the high power system presented in Section V. Fig. 13a presents a constant q_s component of power (*Target IV*), Fig. 13b – sinusoidal unbalanced stator current (*Target V*), Fig. 13c presents a minimum amount of stator current harmonics giving torque oscillations cancellation (*Target VI*). Figures and waveforms of simulation results and experimental results can be compared accordingly – Fig. 13a – Fig. 9, Fig. 13b – Fig. 10, Fig. 13c – Fig. 11. Slight differences between simulation and experiments are visible in all three analyzed targets. More harmonics in the stator current can be seen in the experiment. It is justified by measurement noise in the laboratory test bed, whereas simulation is made with the ideal machine model, so even if grid voltage harmonics occur, the simulation model will give better results (less higher harmonics).

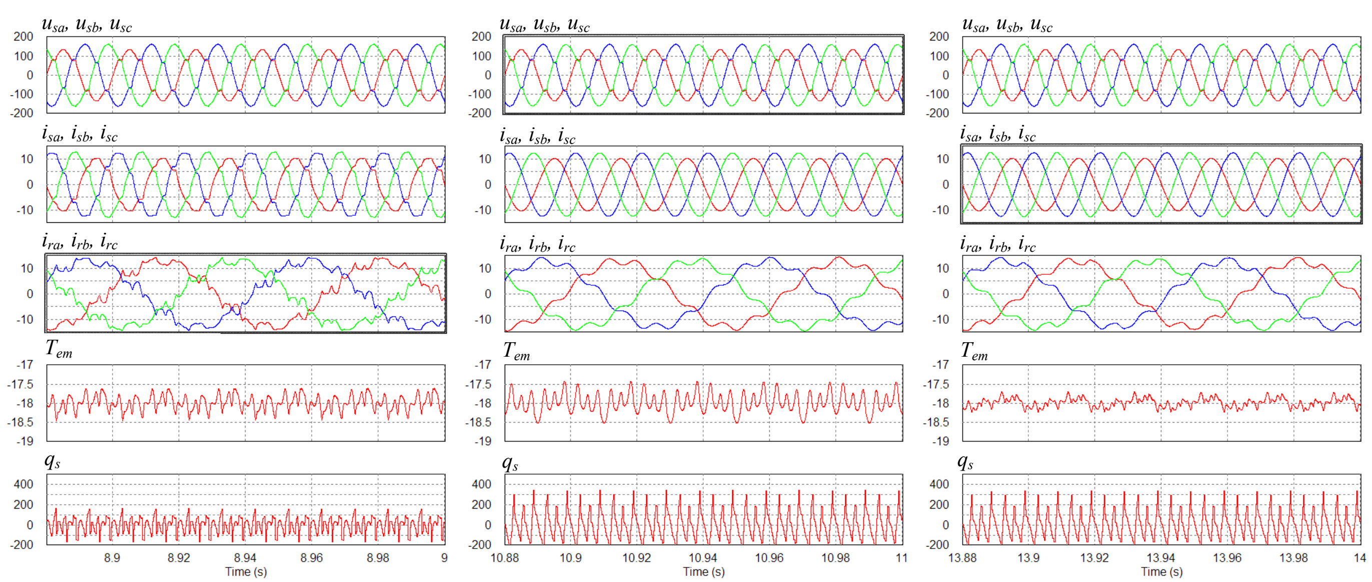

(a) (b) (c)

Fig. 13. Simulation results presenting stator phase voltage u_{sa}, u_{sb}, u_{sc}, stator phase current i_{sa}, i_{sb}, i_{sc}, rotor phase current i_{ra}, i_{rb}, i_{rc}, electromagnetic torque T_{em}, and real q_s component of instantaneous stator power for different targets of torque oscillations cancellation targets a) a constant reference q_s component of power – *Target IV*, b) sinusoidal unbalanced stator current – *Target V*, c) a minimum amount of stator current harmonics giving torque oscillations cancellation – *Target VI*, for the small power machine model with parameters and conditions used in the laboratory test.

1949-3029 (c) 2019 IEEE. Personal use is permitted, but republication/redistribution requires IEEE permission. See http://www.ieee.org/publications_standards/publications/rights/index.html for more information.

This article has been accepted for publication in a future issue of this journal, but has not been fully edited. Content may change prior to final publication. Citation information: DOI 10.1109/TSTE.2019.2935156, IEEE Transactions on Sustainable Energy

VII. Conclusion

The paper compares three targets for elimination or significant reduction of electromagnetic torque oscillations of a doubly fed induction machine operating with unbalanced and distorted grid voltage. Two of the presented targets are new, and they are compared to the target (known in literature) giving torque oscillations compensation with a constant q_s component of instantaneous stator power. Simulation and experimental results have shown that there are no big differences between sinusoidal unbalanced stator current target (elimination of torque oscillations provided by negative sequence only) and minimum stator harmonics giving torque oscillations cancellation (elimination of torque oscillations provided by negative sequence and harmonics) in terms of harmonics content in stator current and torque oscillations. Theoretically (in simulation), introducing a new target with minimum stator current harmonics giving torque oscillations cancellation gives smaller torque oscillations than for purely sinusoidal unbalanced stator current target but this is in a limited range and only if the harmonics occurring in grid voltage have relatively low order, which can be managed by the control system. Torque oscillations for the new targets are comparable (or even a little bit smaller) to the oscillations achieved with the constant q_s stator power target, but give significantly better quality of stator current in terms of stator current harmonics content. However, in the authors' opinion, compensation of torque oscillations produced by harmonics can be neglected in the control system, and only compensation of negative sequence causing oscillations may be taken into consideration. This way, the control structure is simpler (lack of a specially designed multi-band-pass filter for reference current calculation), while the obtained results are still satisfactory. It has to be noted that the presented experimental results have limited representativeness in relation to high power machines, and they are presented mainly to confirm the ability of control practical implementation. To substantiate the simulation results of the high power system presented in the paper, additional simulation results of a small power machine used in a laboratory have been added at the end of the paper.

References

[1] G. Pannell, D. J. Atkinson and B. Zahawi, "Minimum-Threshold Crowbar for a Fault-Ride-Through Grid-Code-Compliant DFIG Wind Turbine," *IEEE Trans. Energy Conv.*, vol. 25, no. 3, pp. 750-759, Sept. 2010.

[2] J. Vidal, G. Abad, J. Arza and S. Aurtenechea, "Single-Phase DC Crowbar Topologies for Low Voltage Ride Through Fulfillment of High-Power Doubly Fed Induction Generator-Based Wind Turbines," *IEEE Trans. Energy Conv*., vol. 28, no. 3, pp. 768-781, Sept. 2013.

[3] A. M. A. Haidar, K. M. Muttaqi and M. T. Hagh, "A Coordinated Control Approach for DC link and Rotor Crowbars to Improve Fault Ride-Through of DFIG-Based Wind Turbine," *IEEE Trans. Ind. Appl.*, vol. 53, no. 4, pp. 4073-4086, July-Aug. 2017.

[4] L. Shang; J. Hu, "Sliding-Mode-Based Direct Power Control of Grid-Connected Wind-Turbine-Driven Doubly Fed Induction Generators Under Unbalanced Grid Voltage Conditions", *IEEE Trans. Energy Conv.*, vol. 27, no. 2, pp. 362-373, June 2012

[5] J. Hu, Y. He, L. Xu, B.W. Williams, Improved Control of DFIG Systems During Network Unbalance Using PI–R Current Regulators, *IEEE Trans. Ind. Electron.*, vol. 56, no. 2, pp. 439- 451, Feb. 2009.

[6] M. Itsaso Martinez, G. Tapia, A. Susperregui and H. Camblong, "DFIG power generation capability and feasibility regions under unbalanced grid voltage conditions", *IEEE Trans. Energy Conv.*, vol. 26, no. 4, pp. 1051-1062, Dec. 2011.

[7] L. Changjin; F. Blaabjerg, C. Wenjie, X. Dehong, "Stator Current Harmonic Control With Resonant Controller for Doubly Fed Induction Generator," *IEEE Trans. Power Electron.*, vol. 27, no.7, pp. 3207-3220, July 2012

[8] G. F. Gontijo, T. C. Tricarico, B. W. Franca, L. F. da Silva, E. L. van Emmerik and M. Aredes, "Robust Model Predictive Rotor Current Control of a DFIG Connected to a Distorted and Unbalanced Grid Driven by a Direct Matrix Converter," *IEEE Trans. Sust. Energy*, 2018 (early access)

[9] J. Hu, H. Nian, H. Xu and Y. He, "Dynamic Modeling and Improved Control of DFIG Under Distorted Grid Voltage Conditions," in *IEEE Trans. Energy Conv.*, vol. 26, no. 1, pp. 163-175, March 2011.

[10] G. Iwanski, T. Luszczyk, P. Pura, and M. Szypulski, "Indirect Torque and Stator Reactive Power Control of Doubly Fed Induction Machine Connected to Unbalanced Power Network," *IEEE Trans. Energy Conv.*, vol. 31, no. 3, pp. 1202–1211, 2016.

[11] G. F. Gontijo, T. C. Tricarico, B. W. Franca, L. F. da Silva, E. L. van Emmerik and M. Aredes, "Robust Model Predictive Rotor Current Control of a DFIG Connected to a Distorted and Unbalanced Grid Driven by a Direct Matrix Converter," *IEEE Trans. Sust. Energy. (early access)*

[12] Y. Wang, Q. Wu, W. Gong and M. P. S. Gryning, "H_∞ Robust Current Control for DFIG-Based Wind Turbine Subject to Grid Voltage Distortions," *IEEE Trans. Sust. Energy*, vol. 8, no. 2, pp. 816-825, April 2017.

[13] M. Szypulski, G. Iwański, "Synchronization of State-Feedback-Controlled Doubly Fed Induction Generator with the Grid", *Bulletin of the Polish Academy of Science – Technical Sciences*, vol. 66, no. 5., pp. 675-685, Oct. 2018

[14] C. Wu and H. Nian, "Stator Harmonic Currents Suppression for DFIG Based on Feed-Forward Regulator Under Distorted Grid Voltage," in *IEEE Trans. Power Electron.*, vol. 33, no. 2, pp. 1211-1224, Feb. 2018.

[15] J. Hu, Y. He, "DFIG wind generation systems operating with limited converter rating considered under unbalanced network conditions– analysis and control design", *Renewab. Energy*, vol. 36, no. 2, pp. 829-847, Feb. 2011.

[16] K. P. Gokhale, D. W. Karraker, S. J. Heikkila, "Controller for a Wound Rotor Induction Machine," U.S. Patent US 6448735 B1, 10.09.2002

[17] I. Villanueva, A. Rosales, P. Ponce and A. Molina, "Grid-Voltage-Oriented Sliding Mode Control for DFIG Under Balanced and Unbalanced Grid Faults," *IEEE Trans. Sust. Energy*, vol. 9, no. 3, pp. 1090-1098, July 2018.

[18] G. Abad, J. Lopez, A. M. Rodriguez, L. Marroyo, G. Iwanski, "Doubly Fed Induction Machine modeling and control for wind energy generation", *IEEE Press Series on Power Engineering*, John Wiley & Sons Inc., IEEE 2011

[19] M. E. Zarei and B. Asaei, "Predictive direct torque control of DFIG under unbalanced and distorted stator voltage conditions," *12th Int. Conf. Environ. and Electr. Eng.*, Wroclaw, 2013, pp. 507-512.

[20] M. I. Martinez, A. Susperregui and G. Tapia, "Second-order sliding-mode-based global control scheme for wind turbine-driven DFIGs subject to unbalanced and distorted grid voltage," *IET Electric Power Applications*, vol. 11, no. 6, pp. 1013-1022, 7 2017.

[21] H. Xu, J. Hu, Y. He,"Integrated Modeling and Enhanced Control of DFIG Under Unbalanced and Distorted Grid Voltage Conditions", *IEEE Trans. Energy Conv.*, vol. 27, no. 3, pp. 725-736, Sept. 2012.

[22] IEEE Recommended Practice and Requirements for Harmonic Control in Electric Power Systems, IEEE Std 519-2014.

Grzegorz Iwanski received the M.Sc. degree in automation and robotics, and the Ph.D. degree in electrical engineering from Faculty of Electrical Engineering at Warsaw University of Technology (WUT), Warszawa, Poland, in 2003 and 2005, respectively. Since January 2006 to December 2008 he was a research worker in the Institute of Control and Industrial Electronics of WUT involved in international project within 6th Framework Programme of EU. Since 2009 he has been an

1949-3029 (c) 2019 IEEE. Personal use is permitted, but republication/redistribution requires IEEE permission. See http://www.ieee.org/publications_standards/publications/rights/index.html for more information.

This article has been accepted for publication in a future issue of this journal, but has not been fully edited. Content may change prior to final publication. Citation information: DOI 10.1109/TSTE.2019.2935156, IEEE Transactions on Sustainable Energy

Assistant Professor in Institute of Control and Industrial Electronics WUT; where in 2019 he received Associate Professor position. He teaches courses on power electronics, drives and power conversion systems. His research interests include variable and adjustable speed power generation systems, photovoltaic and energy storage systems, automotive power electronics and drives. In 2012/2013 he joined the team of REES UPC, Barcelona–Terrassa, within the framework of scholarship of Polish Minister of Science and Higher Education for investigation of power converters topologies with reduced common-mode component for photovoltaic systems. He is co-author of one monograph, three books chapters, and about 60 journal and conference papers. He provided two plenary lectures on IEEE technically sponsored international conferences (EVER'15 and OPTIM-ACEMP'17).

Tomasz Łuszczyk received the M.Sc. degree and the Ph.D. degree, both in electrical engineering from Faculty of Electrical Engineering at Warsaw University of Technology (WUT), Warszawa, Poland, in 2011 and 2017, respectively. Since 2017 he is involved in the project granted by the National Science Centre (Poland) at post-doc position in Institute of Control and Industrial Electronics (WUT). His research is concentrated on vector control of electic machines and grid connected power converters.

Mateusz Piwek received the M.Sc. degree in electrical engineering from Warsaw University of Technology (WUT), Warszawa, Poland, in 2018. His mater thesis has been partially related to this paper. Currently he is an engineer resposnsible for commissioning of high power internal combustion engine based generation and co-generation systems in polish company HORUS Energia Sp. z o.o.

1949-3029 (c) 2019 IEEE. Personal use is permitted, but republication/redistribution requires IEEE permission. See http://www.ieee.org/publications_standards/publications/rights/index.html for more information.